British Columbia Geological Survey
Geological Fieldwork 1995

PRELIMINARY PETROGRAPHIC, GEOCHEMICAL AND FLUID INCLUSION STUDIES OF THE FORS DEPOSIT, SOUTHEASTERN BRITISH COLUMBIA (82G/5W)

Craig H.B. Leitch, Consulting Geologist

KEYWORDS: Economic geology, sedex deposits, base metals, vein, hydrothermal alteration, Fors, Vine, Sullivan, Purcell Supergroup, Aldridge Formation, Moyie sills.

INTRODUCTION

At the Fors property, argentiferous lead-zinc sulphide mineralization consisting of pyrrhotite, sphalerite, galena, arsenopyrite, pyrite, chalcopyrite and rare native bismuth occurs in stratiform, semimassive to massive lenses, disseminations and veins at the top of a discordant zone of pebble wacke or fragmental in middle Aldridge sandstone and mudstone (Britton and Pighin, 1995). This preliminary description of the petrography, geochemistry and fluid inclusions is based entirely on examination of drill-core specimens collected by the writer, R.J.W. Turner of the Geological Survey of Canada, J.M. Britton (formerly of the B.C. Geological Survey Branch) and D.L. Pighin of Consolidated Ramrod Gold Corporation. This paper builds on the geological description in Britton and Pighin (1995).

GEOLOGICAL SETTING

The Fors prospect (MINFILE 082GSW035) is located near Moyie Lake, 17 kilometres southwest of Cranbrook (Figure 1) and 8 kilometres southwest of the Vine prospect, a Middle Proterozoic massive sulphide base and precious metal vein deposit (Höy and Pighin, 1995). Access to the Fors and Vine properties is by paved and gravel roads from Highway 3/95. The exploration history of the Fors property is summarized by Britton and Pighin (1995).

Hostrocks to the Fors and Vine deposits are mainly siliciclastic and lesser carbonate sedimentary rocks of the Aldridge Formation of the Middle Proterozoic Purcell Supergroup, exposed in a major northeasterly plunging anticlinorium cut by high-angle normal and reverse faults (Figure 1; Höy, 1993). The formation comprises in excess of 4000 metres of turbidites probably deposited in an extensional basin in an intracratonic setting (Winston *et al.*, 1984), and consists of three divisions. The lower Aldridge (base not exposed) consists mainly of thin-bedded rusty argillaceous siltstone and is overlain by 3000 metres of thick to thin-bedded turbidites of the middle Aldridge and 500 metres of massive to faintly laminated argillite of the upper Aldridge (Höy, 1993). At the Fors, the top of the lower Aldridge is marked by a concordant pebble wacke or fragmental that is stratigraphically equivalent to the Sullivan horizon (Figure 2; Britton and Pighin, 1995). A number of thick gabbro sills (Moyie sills) intrude the upper part of the lower Aldridge and the middle of the middle Aldridge, with contact features indicating intrusion into wet, partly consolidated sediments (Höy, 1989). Uranium-lead dating of zircons from these sills (1445±11 Ma, Höy, 1989; 1467 Ma, Anderson *et al.*, in preparation) therefore constrain the Proterozoic age of the Purcell basin and its contained mineral deposits.

The Fors area is underlain by gently to moderately north to northeast-dipping strata that mostly show only gentle open folds and are cut by the major northeast-striking Moyie fault and minor northwest-striking high-angle faults (Figure 1). Metamorphic grade, attributed to burial, is middle greenschist facies (McMechan and Price, 1982), with estimates of temperature and pressure for the Sullivan mine area of 440±50 °C and 3±1 kilobars (De Paol and Pattison, 1993) or 375 °C and 4.5±1 kilobars (Lydon and Reardon, 1993). Regional deformation and metamorphism occurred at about 1350 Ma based on lead-lead dating of sphene from the Sullivan deposit and adjacent rocks (Schandl *et al.*, 1993). Compression and as much as 300 kilometres of eastward translation occurred during the Jura-Cretaceous (Price, 1981), and the area has beeen subjected to Eocene extensional faulting.

Most of the altered rocks described below belong to the middle Aldridge Formation, and consist mainly of detrital quartz and lesser but significant feldspar (up to 20%: Edmunds, 1977), with variable amounts of porphyroblastic biotite, white mica (muscovite and sericite), chlorite, sulphides (pyrrhotite and pyrite), and accessory sphene, allanite, apatite and zircon (Leitch *et al.*, 1991).

HYDROTHERMAL ALTERATION

Several unusual alteration assemblages are associated with the Fors deposit, either closely or loosely related to the sulphide mineralization. Although these assemblages are all now composed of metamorphic minerals, they presumably developed after distinctive precursor minerals, as has been documented for the Sullivan deposit (Leitch and Turner, 1992; Shaw *et al.*, 1993a,b). The Fors deposit is crudely mushroom shaped (Figure 2; Britton and Pighin, 1995), with the stem consisting of a tourmaline and plagioclase-altered zone within and around the fragmental pipe, and the cap composed of plagioclase-biotite, calcsilicate (actinolite-talc) and mica (biotite-muscovite) alteration assemblages with disseminated to bedded sulphides. Both the stem and the cap are cut by a late-stage, sulphide-rich vein. Following the scheme adopted by and illustrated in hand

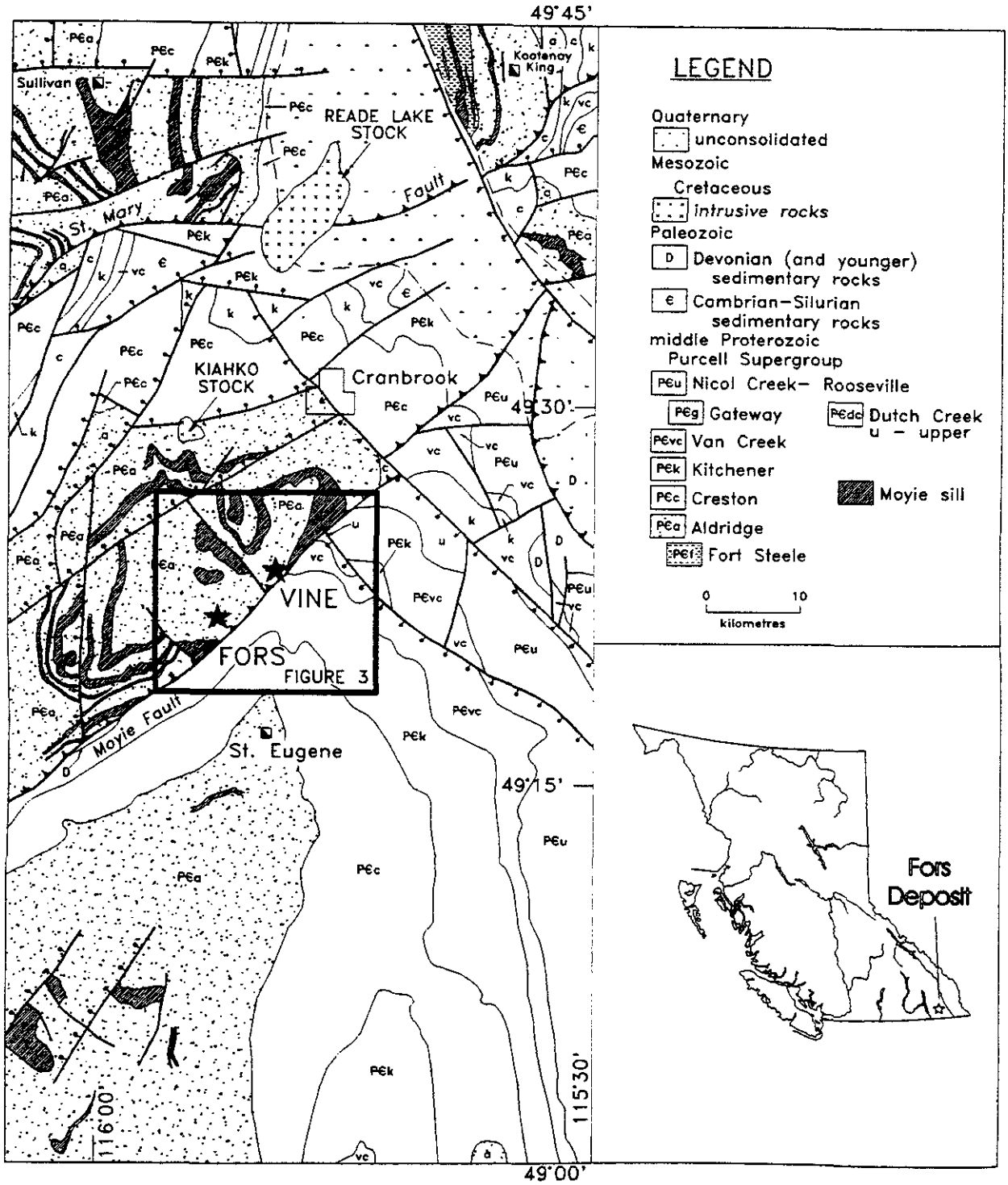

Figure 1. Regional geology and deposit location.

specimen in Britton and Pighin (1995), the alteration types are grouped into five main associations: tourmaline; plagioclase-biotite-garnet; biotite-calcsilicate; sericite; and silica (Figure 2). The petrographic descriptions in this paper are intended to complement the field descriptions in Britton and Pighin.

DESCRIPTION OF SAMPLES AND ANALYTICAL PROCEDURE

The samples selected for this study are mainly from diamond-drill holes 92-1 and 92-2 (located in section on Figure 2), and two from diamond-drill hole 93-10 to examine peripheral alteration. Thin and polished thin sections

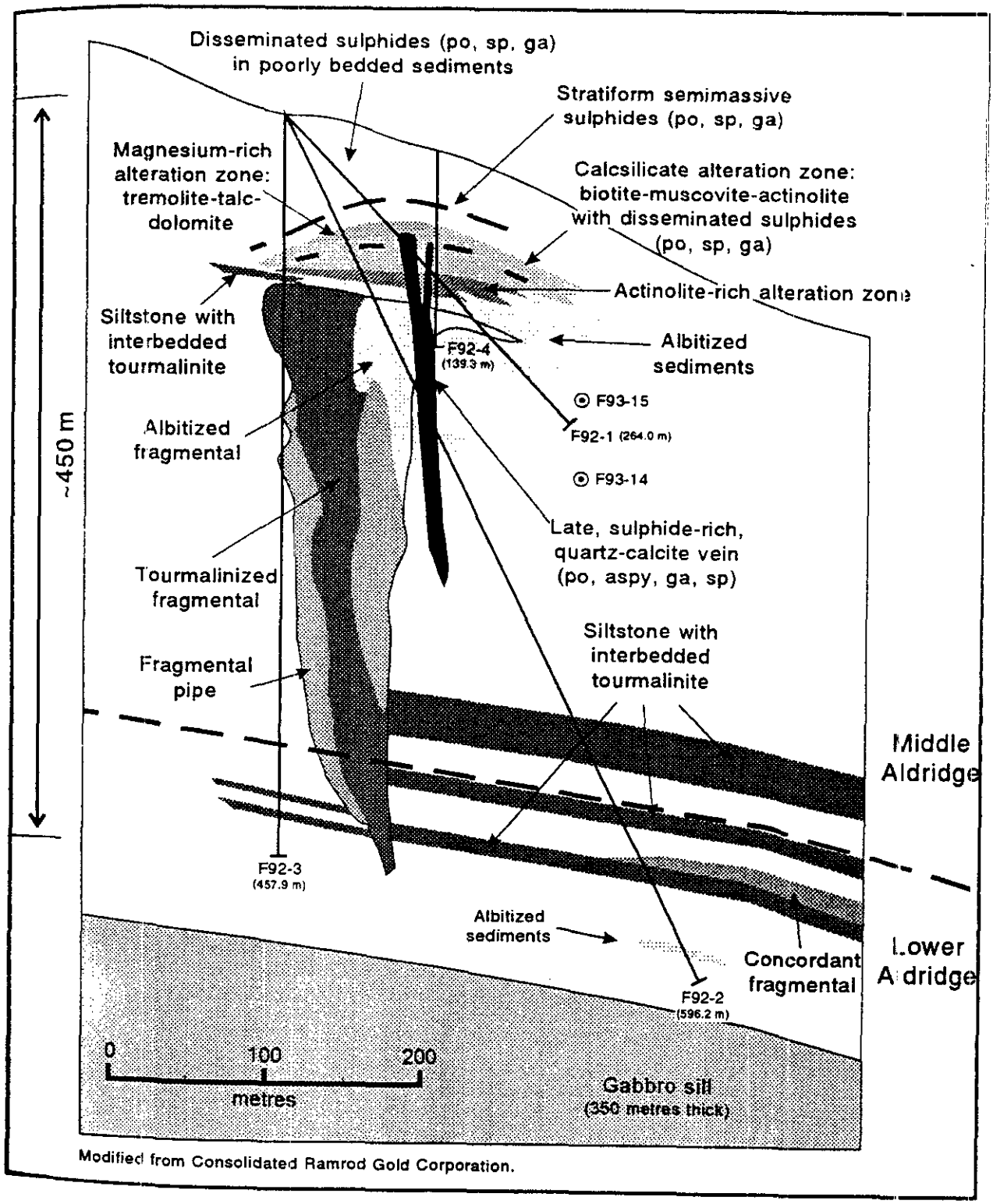

Figure 2. Schematic cross-section, Fors deposit, to show location.

were cut from drill core and examined in transmitted and reflected light and by SEM-EDS (scanning electron microscope - energy dispersive microanalysis). Photographs of hand samples representative of the various alteration types are in Britton and Pighin (1995).

Geochemical analyses on related samples (single offcuts of drill core) were completed for 37 elements [Ag, Al, As, Au, B, Ba, Be, Bi, Ca, Cd, Co, Cr, Cu, Fe, Hg, K, La, Mg, Mn, Mo, Na, Nb, Ni, P, Pb, Sb, Sc, Sn, Sr, Th, Ti, U, V, W, Y, Zn and Zr by HF digestion - ICP (inductively coupled plasma)] at Acme Laboratories, for major oxides SiO_2, Al_2O_3, TiO_2, Fe_2O_{3t}, MnO, MgO, CaO, Na_2O, K_2O, loss on ignition, carbon, sulphur (S_t) and barium by fused disk XRF (x-ray fluorescence) and Leco induction furnace at Cominco Exploration Research Laboratory, plus arsenic, antimony and mercury by atomic absorption at Chemex Labs Ltd., and boron by neutron activation by Activation Laboratories Ltd., all under the direction of Ray Lett of the British Columbia Geological Survey Branch.

Following initial petrographic studies, doubly polished sections 50 to 100 microns thick were prepared by standard methods (Holland *et al.*, 1978) for those samples chosen for fluid inclusion microthermometry. A USGS (United States Geological Survey) gas-flow heating and freezing stage, calibrated in accordance with the manufacturer's recommendations, was used to make microthermometric measurements. The accuracy when so calibrated is better than ±0.4°C from -56.6 to +660.4°C (T.J. Reynolds, unpublished manuscript, 1988). Precision was estimated by replicate measurements to be ±1% up to 200°C and ±2% from 200 to 500°C.

PETROGRAPHY

Tourmalinization consists of very fine needles of tourmaline replacing feldspar and mica interstitial to the detrital quartz framework in the siltstones. This is characteristic of tourmalinization whether it is of the dark black (bedded) or light brown (discordant fragmental) type. The first type, probably the oldest, is overprinted by most other types of alteration; also, tourmalinized argillite occurs as contorted rip-up clasts in siltstone, and rare dark tourmaline clasts are present in the discordant fragmental (Britton and Pighin, 1995).

An example of the first type (F92-2 422 m) consists of detrital quartz (< 60 μm) and 10-50% pale greenish brown tourmaline (1-5 by 10-50 μm), with scattered large, euhedral white, to pink garnets to several millimetres in diameter. In contrast to similar fine hydrothermal tourmaline at the Sullivan deposit with Fe/(Fe+Mg), or F/M, ratios about 0.4 to 0.5, Fors tourmaline appears more iron rich (probably schorlitic; Fe:Si peak height ratio of 0.72 sugesting F/M ratio of perhaps 0.6 to 0.7). The garnets are anisotropic and strongly sieved by inclusions of quartz, tourmaline and sphene (the same minerals as in the matrix). The garnet is manganese rich, particularly at the core (Mn:Fe peak height ratio of 1.37). Note that SEM study permits only qualitative analysis, but the garnets from Fors are comparable to garnets from the Sullivan deposit analysed by microprobe which have manganese contents of up to 80 mol % spessartine (Leitch, 1992a). Accessories inlcude sphene (containing minor ilmenite and rutile) and traces of allanite with Ce>Nd>La>Sm, as at Sullivan. The tourmalinite is cut by bedding-parallel veins of quartz-zoisite±muscovite, pyrrhotite, calcite, sphene, arsenopyrite, minor sphalerite and rare galena, and late bedding-perpendicular veins of quartz, Ca-K zeolite, and minor hydrobiotite and pyrite around pyrrhotite, sphalerite, galena and traces of native bismuth.

Examples of the second type are from 277.2 and 281.1 metres in the same hole, in which grey and brown tourmalinite composed of 2x20 micron pale brown tourmaline alternates with 2 to 5 millimetre thick layers of coarser (possibly recrystallized, to 50 μm) deeper brown tourmaline-potassium feldspar-muscovite-garnet and rare 1 to 2-millimetres laminae of reddish brown tourmalinite rich in sphalerite (10 μm, 15%) that also contain up to 15% apatite (to 60 μm), 5% galena (10 μm) and traces of native bismuth (2-5 μm). Detrital quartz is absent in these laminae. The tourmaline appears to be slightly less iron rich (Fe:Si peak height ratio of 0.63) than in the black tourmalinite; garnet is isotropic but pink and similarly manganese rich (Mn:Fe peak height ratio of 1.27). The potassium feldspar appears to be microcline. Bedding-parallel veins consist of pyrrhotite (with minor pyrite in places), sphalerite, chalcopyrite, quartz, zoisite and muscovite and are crosscut by bedding-perpendicular veinlets of green hydrobiotite and calcium (plus minor K and Mg)-bearing zeolite.

Tourmaline also occurs in unusual stylolite-like "veins" with white and pink or pale grey-green envelopes at 155 to 156 metres in hole F92-1. The tourmaline is a pale brown intermediate schorl-dravite with less iron than tourmaline in the fine tourmalinite and lower, variable calcium content compared to tourmalines analysed at Sullivan (Leitch *et al.*, in preparation a). These relationships indicate recrystallization of the tourmaline in the "veins". The white envelopes are composed of feldspar, mainly plagioclase, probably of albite-oligoclase composition (Ca:Na peak heights of about 4:1 to 10:1), significant potassium feldspar or in places secondary quartz, and minor zoisite-clinozoisite (in places containing minor enrichment in rare-earth elements). The plagioclase forms subhedral crystals ranging from fine (0.1 mm) to coarse (0.5-1.0 mm) replacing the original detrital framework of the rock; potassium feldspar is similarly coarse and probably not detrital. Thus white areas can be due to alteration by albite-oligoclase, potassium feldspar or quartz (silicification). The pink coloration is due to fine shreddy biotite (0.1-0.2 mm) and unusually abundant sphene; grey-green colour is due to sericite (50 μm muscovite) that appears to replace fine-grained (but not coarse) albite-oligoclase, with implications for the timing of sericitization (see below).

Plagioclase (± biotite) alteration, well exposed in hole F92-1 from 163 to 178 metres, forms a fine sugary white to pink or pale brown rock with significant replacement of the detrital framework by feldspar; the pink to brown colour is due to fine biotite and lesser sphene. Detrital quartz appears to be recrystallized to 0.25-millimetre anhedra. There is generally variable muscovite and minor zoisite

present, and accessory pyrrhotite, apatite and zircon. Coarser clots, layers and veins are composed of alkali feldspar (plagioclase and potassium feldspar in variable proportions) and quartz to 1 millimetre diameter, plus minor biotite, muscovite, chlorite, zoisite, pyrrhotite and sphene. White alteration envelopes in these rocks are composed of plagioclase, surrounding fractures filled with zoisite, pyrrhotite, minor muscovite, quartz, sphene with rutile cores, chlorite and rare, pale coloured tourmaline. Carbonate, zoisite and sericite outside the veinlet envelopes may be after former detrital feldspars. "Clots" in the rock consist of zoisite, chlorite, greenish brown tourmaline (probably intermediate schorl-dravite), minor carbonate, sphene and pyrrhotite together with an unidentified bladed mineral with high relief, moderate birefringence and chemistry intermediate between tremolite and zoisite.

These rocks are also cut by narrow, irregular, anastamosing veinlets of sphene, up to 0.3 millimetre thick with traces of allanite and borders of magnesium-rich chlorite (chlorite in these rocks contains significant manganese and has low F/M, about 0.25-0.4, based on optical characteristics and SEM analysis: *cf.* type 0/1 chlorite described at Sullivan by Leitch *et al.* (in preparation a). Sphene veinlets have a dark stylolitic appearance in hand specimen, and are cut by 0.2-millimetre veinlets of a bladed, low relief, low birefringence mineral that is probably zeolite (identified as Ca ± Na, K Al-silicate by SEM).

The composition of plagioclase varies from albite to oligoclase and lesser andesine or even labradorite, based on optical tests (extinction angles where possible, comparison of relief to quartz) supported by SEM analysis which shows Ca:Na peak heights up to 50:1. A sample from the core of a plagioclase-rich zone, 50 metres thick (F92-1 166.5 m, logged as "albitized"), contains major potassium feldspar in addition to plagioclase, with approximate composition ranging from albite-oligoclase to andesine (Ca:Na peak height ratios determined by SEM about 7:1 to 50:1). At the borders of such plagioclase-rich zones, plagioclase in veinlets cutting calcite-rich samples ("skarn" or calcsilicate rocks, *e.g.* F92-2 176.9 m) is very calcic, possibly anorthite with Ca:Na peak height ratios of over 100:1. Above the plagioclase-rich zone in F92-2, similar calcic plagioclase (Ca:Na peak heights over 50:1) is also found in veinlets that cut tremolitic amphibole, but are cut by fractures of zoisite-sulphide-muscovite-calcite (at 70.7 and 98.9 m) or by coarse white quartz (102.4 m).

Biotite alteration is distinctive at Fors (it is not known at Sullivan), occurring as envelopes to sulphide-bearing veins and larger zones, generally fringing calcsilicate (tremolite/actinolite-talc) alteration, especially in the cap zone to the deposit (Britton and Pighin, 1995). Biotite forms coarse euhedral flakes to 2 millimetres in diameter that contain inclusions of magnesium-rich (type 0) chlorite and are slightly altered to more iron-rich (type 1/2) chlorite (classifications of chlorite developed at the Sullivan deposit: Leitch *et al.*, in preparation a). Semiquantitative SEM-EDS analysis of the biotites from Fors suggests they are iron, magnesium, and titanium rich. In contrast to macroscopic relations noted by Britton and Pighin (1995), in thin section, tremolite and actinolite appear to be replaced by biotite and quartz, possibly because petrographic observations focus on the results of metamorphic reactions rather than the original hydrothermal relationships. Sphene, zoisite and garnet, and traces of allanite, are also common in the veins with sulphides, which include pyrrhotite, arsenopyrite, sphalerite, galena, chalcopyrite and rare pyrite. As at Sullivan, minerals such as sphene, zoisite, garnet and allanite (or their metamorphic precursors) appear to be closely associated with the hydrothermal mineralizing process.

Garnetiferous rocks are mainly found with plagioclase alteration and in sulphide-bearing veins. In the former, garnets form large, rounded to subhedral aggregates or zoned crystals up to 7 millimetres in diameter, with cores more densely sieved than the rims by minute (10-15 μm) inclusions of the same silicates in the rock matrix around them (quartz, plagioclase, sphene). Alternatively, garnet occurs as subhedral skeletal 1 millimetre crystals with biotite, carbonate, quartz, pyrrhotite, tremolite, zoisite, sphene and allanite, in curious orbicular structures up to 1 centimetre across. In veins, garnet occurs as subhedral to euhedral crystals up to 1 millimetre in diameter with the same minerals as in the orbicular structures. Garnet is also present in the major sulphide-rich quartz-calcite vein (Figure 2) and its calcite-rich envelopes (F92-2 221.4 m). The garnet is probably spessartine rich, based on comparison of SEM-EDS analyses (Mn:Fe peak height ratios generally 1 to 1.5) with SEM anlyses of similar garnets from Sullivan subjected to microprobe analysis. Crystal rims are slightly enriched in manganese in some samples. In places, garnet is partly replaced by carbonate (mainly Mn-calcite, but Mn-siderite, found rarely, could be pseudomorphic after garnet).

Tremolite/actinolite-talc alteration is concentrated in a cap zone over the deposit that ranges from a core of actinolite-rich rocks to a fringing calcsilicate alteraton zone (biotite-muscovite-tremolite-actinolite-calcite-zoisite, with disseminated sulphides including pyrrhotite, sphalerite, and galena) and an upper magnesium-rich alteration zone consisting of tremolite, talc and dolomite (Figure 2). Amphibole in these alteration zones is generally coarse grained, occurring as ragged subhedral crystals up to 5 millimetres long. Composition varies from a dark green actinolite (Mg:Fe peak height ratio about 1.6) in the core zone to pale green tremolite (Mg:Fe peak height ratio about 2.8) in the fringing zones. Petrographically, amphibole appears to be replaced by carbonate and biotite, and is cut by calcic plagioclase and quartz; in places, it contains inclusions of biotite, sphene and pyrrhotite. However, macroscopically, amphibole is described as replacing biotite (Britton and Pighin, 1995).

Sericitization occurs pervasively as a distal aureole around the other alteration assemblages at depth and above the bedded sulphide zone, where it is associated with silicification (Britton and Pighin, 1995). It may be distinguished in the field by its grey-green colour and softness (drill core of sericitic alteration is mostly scratched by steel, unless it occurs in quartz-rich units). In thin section sericite (fine-grained muscovite) occurs as euhedral to subhedral flakes

TABLE 1
GEOCHEMISTRY OF ALTERED ROCKS

	Element	CaO	K_2O	P_2O_5	SiO_2	Al_2O_3	MgO	Na_2O	Fe_2O_3	TiO_2	MnO	LOI	Total	Ba	As	Hg	Sb	B
	Units	%	%	%	%	%	%	%	%	%	%	%	%	ppm	ppm	ppb	ppm	ppm
	Method	XRF	XRF	XRF	XRF	XRF	XRF	XRF	XRF	XRF	XRF	FUS	SUM	XRF	HAA	CAA	EAA	INA
	Laboratory	COM	COM	COM	COM	COM	COM	COM	COM	COM	COM	COM	COM	COM	CME	CME	CME	ACT
	Detection Limit	0.01	0.01	0.01	0.01	0.01	0.01	0.01	0.01	0.01	0.01	0.01	0.01	1	1	10	0.2	2
Lab.No	Field No.																	
49444	F92-1 63	3.49	1.36	0.04	75.53	8.79	1.72	0.2	4.11	0.31	0.43	2.32	98.3	197	1	20	2.8	4
49445	F92-1 72.2	1.84	3.57	0.09	68.49	12.79	3.66	1.11	5.18	0.47	0.13	1.81	99.14	1605	1	10	0.8	430
49446	F92-1 76.0	13.59	0.31	0.05	50.23	2.77	17.31	0.2	8.38	0.09	0.88	3.82	97.63	21	8	10	10.5	9
49447	F92-1 141.1	5.33	3.19	0.08	68.9	16.24	0.64	2.44	1.01	0.58	0.11	0.99	99.51	680	296	10	1.4	35
49448	F92-1 166.4	6.19	0.22	0.07	64.33	21.01	0.1	6.36	0.24	0.72	0.02	0.44	99.71	57	360	10	1.6	19
49449	F92-1 173.3	2.3	1.11	0.04	84.02	7.31	0.32	1.25	2.02	0.27	0.07	0.79	99.51	259	30	10	0.6	46
49450	F92-2 105.2	1.75	2.54	0.03	83.84	7.36	0.43	0.33	0.49	0.24	0.03	0.85	97.89	1100	560	10	4.4	255
49451	STD - FER 3	2.14	0.29	0.13	49.84	1.55	1.26	0.1	40.21	0.07	0.19	3.7	99.48	59	26	40	3.8	83
49452	F93-10 39.2	1.67	3.96	0.1	66.06	13.95	4.23	1.31	5.33	0.52	0.15	2	99.28	869	1	10	0.8	105
49453	F93-10 44.1	23.63	0.21	0.05	7.06	4.82	21.48	0.05	3.93	0.2	0.86	36.81	99.1	4	2	40	1.4	3
49454	F93-10 49.3	15.25	0.04	0.04	20.83	5.88	25.42	0.02	2.91	0.2	0.4	28.41	99.4	2	1	20	1	<2
49455	F93-10 56.7	3.94	0.3	0.05	37.91	14.26	27.13	0.05	6.3	0.6	0.29	8.95	99.79	29	1	10	0.4	<2
49456	F93-10 59.8	0.83	9.06	0.07	41.2	14.89	20.69	0.04	8.16	0.54	0.27	3.88	99.63	388	2	30	0.8	2
49457	F93-10 64.4	12.5	0.74	0.05	53.66	15.2	8.63	0.63	5.32	0.48	0.46	1.59	99.26	55	1	10	0.6	5
49458	F93-10 69.7	8.06	1.93	0.06	58.45	17.17	4.19	2.18	3.46	0.62	0.22	1.97	98.31	232	64	10	1.2	52
49459	F93-10 73.2	3.93	1.07	0.03	81.39	6.41	2.23	0.63	2.24	0.22	0.17	1.04	99.37	327	1020	20	2.8	<2

	Element	Mo	Cu	Pb	Zn	Ag	Ni	Co	Mn	Fe	As	U	Th	Sr	Cd	Sb	Bi	Sc
	Units	ppm	ppm	ppm	ppm	ppm	ppm	ppm	ppm	%	ppm	ppm	ppm	ppm	ppm	ppm	ppm	ppm
	Method	TICP	TICP	TICP	TICP	TICP	TICP	TICP	TICP	TICP	TICP	TICP	TICP	TICP	TICP	TICP	TICP	TICP
	Laboratory	ACM	ACM	ACM	ACM	ACM	ACM	ACM	ACM	ACM	ACM	ACM	ACM	ACM	ACM	ACM	ACM	ACM
	Detection Limit	2	2	5	2	0.3	2	2	5	0.01	5	10	2	2	0.4	5	5	1
Lab.No	Field No.																	
49444	F92-1 63	2	115	1331	929	1.3	11	3	3568	2.98	<4	<10	7	178	5.4	6	4	9
49445	F92-1 72.2	2	66	90	204	<0.3	18	5	915	3.65	<4	<10	7	167	0.4	5	<5	12
49446	F92-1 76.0	5	23	6358	6215	9.1	10	6	5618	5.63	8	<10	<2	32	46.4	16	18	2
49447	F92-1 141.1	<2	4	58	222	<0.3	15	5	475	0.76	45	<10	12	264	1.9	<5	<5	12
49448	F92-1 166.4	2	<2	28	11	<0.3	4	3	86	0.15	50	<10	11	317	0.6	<5	<5	3
49449	F92-1 173.3	2	18	21	14	<0.3	8	2	456	1.48	<4	<10	5	56	<0.4	<5	<5	5
49450	F92-2 105.2	<2	<2	39	13	<0.3	9	6	168	0.43	174	<10	6	49	<0.4	5	<5	5
49451	Std. - FER 3	14	41	64	216	0.5	57	15	934	4.99	29	<10	12	400	1.2	10	6	14
49452	F93-10 39.2	2	35	64	184	<0.3	21	8	976	3.67	<4	<10	9	155	0.6	9	<5	12
49453	F93-10 44.1	<2	16	66	148	<0.3	11	4	5414	2.76	<4	<10	5	531	<0.4	14	<5	4
49454	F93-10 49.3	<2	4	15	128	<0.3	18	4	2624	1.87	<4	<10	5	719	0.5	16	<5	5
49455	F93-10 56.7	<2	4	13	254	<0.3	20	8	1930	3.76	<4	<10	6	12	<0.4	11	<5	5
49456	F93-10 59.8	2	4	8	471	<0.3	29	8	1765	5.3	<4	<10	11	5	0.7	11	<5	11
49457	F93-10 64.4	12	<2	196	299	0.9	25	2	3007	3.74	<4	<10	11	303	0.4	<5	<5	10
49458	F93-10 69.7	<2	<2	520	383	2.5	20	1	1571	2.52	34	<10	13	377	2.3	8	7	14
49459	F93-10 73.2	6	6	103	116	0.5	8	3	1032	1.66	102	<10	6	91	<0.4	8	4	4

	Element	V	Ca	P	La	Cr	Mg	Ba	Ti	Al	Na	K	W	Zr	Sn	Y	Nb	Be
	Units	ppm	%	%	ppm	ppm	%	ppm	%	%	%	%	ppm	ppm	ppm	ppm	ppm	ppm
	Method	TICP	TICP	TICP	TICP	TICP	TICP	TICP	TICP	TICP	TICP	TICP	TICP	TICP	TICP	TICP	TICP	TICP
	Laboratory	ACM	ACM	ACM	ACM	ACM	ACM	ACM	ACM	ACM	ACM	ACM	ACM	ACM	ACM	ACM	ACM	ACM
	Detection Limit	2	0.01	0.01	2	2	0.01	1	0.01	0.01	0.01	0.01	2	2	2	2	2	1
Lab.No	Field No.																	
49444	F92-1 63	24	2.43	0.014	25	198	1.12	218	0.19	4.88	0.23	1.16	3	24	15	18	9	1
49445	F92-1 72.2	46	1.23	0.035	23	101	2.21	1631	0.28	6.93	0.77	2.78	5	55	26	19	11	2
49446	F92-1 76.0	28	8.4	0.005	7	13	29.67	47	0.05	1.96	0.11	0.22	<2	13	33	6	1	<1
49447	F92-1 141.1	28	3.9	0.027	18	103	0.46	581	0.34	9.11	1.52	1.88	<2	35	29	27	14	2
49448	F92-1 166.4	8	4.11	0.02	7	45	0.06	38	0.39	10.08	3.43	0.12	10	39	43	35	19	2
49449	F92-1 173.3	18	1.59	0.012	22	133	0.23	223	0.15	3.88	0.79	0.78	2	32	9	15	6	1
49450	F92-2 105.2	14	1.14	0.009	16	191	0.18	1034	0.12	3.63	0.22	1.98	2	26	24	15	6	<1
49451	Std. - FER 3	75	2.76	0.124	42	76	2.06	530	0.36	8.86	1.03	1.51	17	46	<2	21	18	4
49452	F93-10 39.2	46	1.13	0.043	32	84	2.86	813	0.29	7.65	0.74	2.69	7	63	11	23	12	2
49453	F93-10 44.1	14	14.84	0.007	1	13	40.47	19	0.04	3.69	0.01	0.21	3	12	2	9	5	<1
49454	F93-10 49.3	16	10.58	0.01	13	15	44.21	5	0.01	4.26	0.01	0.01	2	17	<2	11	5	<1
49455	F93-10 56.7	37	2.73	0.019	46	39	33.71	12	0.05	7.96	0.04	0.19	8	28	2	18	8	<1
49456	F93-10 59.8	47	0.38	0.026	36	36	29.77	418	0.31	10.25	0.03	5.6	3	68	6	12	12	<1
49457	F93-10 64.4	36	7.87	0.01	47	76	14.91	64	0.27	8.94	0.32	0.48	2	35	23	30	9	2
49458	F93-10 69.7	52	5.29	0.017	32	101	3.56	230	0.32	9.41	1	1.24	5	51	14	25	14	3
49459	F93-10 73.2	14	2.76	0.008	18	181	1.44	293	0.12	3.49	0.38	0.72	2	19	11	12	7	<1

NOTES:

XRF = Fused disc-X-ray fluorescence spectroscopy

FUS = Fusion at 1050°C

SUM = Sum of oxides

HAA = Aqua regia digestion - hydride generation atomic absorption spectroscopy

CAA = Aqua regia digestion-flameless atomic absorption spectroscopy

EAA = HCl-$KClO_3$ digestion - atomic absorption spectroscopy

INA = Thermal neutron activation analysis

TICP = $HClO_4$-HNO_3-HCl-HF-Digestion-Inductively Coupled Plasma Emission Spectroscopy

COM = Cominco Research Laboratory

CME = Chemex Laboratories Ltd.

ACM = ACME Analytical Laboratories Ltd.

ACT = Activation Laboratories Ltd.

generally less than 50 microns in diameter, making up to 65% of argillaceous hostrocks but as little as 25% of quartz-rich hostrocks such as siltstones (*e.g.*, hole F93-10, peripheral to the main mineralized zone; not on Figure 2). Sericite-altered layers also occur within the central deposit area, interbedded with tourmalinite and albite-altered rocks. In thin sections from these areas, sericite appears to replace feldspars, including original detrital plagioclase and potassium feldspar, some secondary plagioclase (albitic to calcic in composition), and layers of possibly secondary potassium feldspar.

Minor muscovite, as euhedral flakes up to 0.5 millimetre in diameter, is also found as a probable hydrothermal mineral in many veins with sulphide, zoisite, biotite, tourmaline and sphene, although in places it may possibly be the product of alteration of biotite (with chlorite). Some of these muscovite-bearing veins have plagioclase-biotite envelopes; sericite does not appear to replace albitized rocks. However, pale green sericitic envelopes around sulphide-bearing veins do appear to cut potassium feldspar altered or silicified rocks.

Silicification has been described by Britton and Pighin (1995) as occurring in two ways: first, as irregular zones apparently confined to strata overlying the calcsilicate alteration cap, up to the level of the Main showing (Maheux, 1990) or elsewhere in drill core (Klewchuck, 1993), and secondly, as thin envelopes around chalcedonic (?late-stage) quartz veins.

Silicification is difficult to discern reliably in both hand specimen and thin section. Zones of white to pale grey rock, either as envelopes to fractures or veins, or forming pervasive zones, variably identified as silicification or albitization in hand specimen, can turn out on petrographic/SEM examination to be secondary albite, calcic plagioclase, potassium feldspar, or quartz (silicification). In some cases both feldspathic and silicic alteration are present.

In the present study, pervasive secondary (possibly hydrothermal) quartz was identified mainly on the basis of its recrystallized texture, which contrasts with the more rounded outlines of the ubiquitous detrital quartz. This is similar to the textures observed at Sullivan; in contrast to earlier statements (*e.g.* Leitch *et al.*, 1991) that discounted the introduction of quartz due to alteration, it now appears likely that silicification is more widespread at both Fors and Sullivan (Leitch *et al.*, in preparation a). Note that in most of the Fors calcsilicate alteration, the detrital quartz framework is entirely absent; minor quartz occurring with calcsilicate alteration is clearly secondary, and largely appears to replace amphibole.

White alteration envelopes around narrow tourmaline-bearing veins in plagioclase-altered sediments (F92-1 between 150 and 170 m: loosely termed "albitized sediments" in Figure 2) consist of either silicification (euhedral to subhedral crystals of 0.1-0.2 mm diameter) or feldspar alteration (subhedral 0.5-1.0 mm plagioclase mixed in places with anhedral potassium feldspar to 0.5 mm). In thin sections lacking a polished surface (so that SEM studies are not possible), the lack of optical relief between quartz and secondary albite-oligoclase (generally untwinned) makes it impossible to tell silicification and plagioclase alteration apart, even petrographically.

GEOCHEMISTRY

As part of a preliminary assessment of the geochemistry of alteration, various alteration types were characterized by major oxides (SiO_2, Fe_2O_{3t}, MnO, MgO, CaO, Na_2O, K_2O, H_2O, C, S_t) and trace elements (Ag, As, B, Ba, Bi, Cu, Hg, La, Pb, Sb, Sn, Zn), uncorrected for volume changes, considered most likely to reflect alteration processes. Other oxides (Al_2O_3 and TiO_2) and trace elements (Nb, Y, Zr) are relatively immobile and may be used to estimate the amount of volume change during alteration, using the average chemistry of unaltered host sediments as a starting point. Geochemical data are in Table 1.

Actinolite-talc alteration is represented by samples F92-1 76 (actinolite rich), F93-10 56.7 (tremolite rich) and F93-10 64.4 (silicified, plagioclase altered). This alteration is characterized by high magnesia (to 27%, particularly in those richest in talc) and lime (to 14%). Silica values are low, as low as 7% in rocks made up mainly of carbonate, to 50% in those made up mainly of amphibole or 55% in the silicified example. Alumina and titania vary from extremely low (as low as 3% and 0.1%, respectively) in the samples rich in amphibole and talc, to normal (15% and 0.5%, respectively: Leitch *et al.*, in preparation b) in the samples that include significant muscovite or biotite. This probably indicates significant volume addition in the case of the amphibole or talc-rich samples, and is confirmed by low contents of zirconium, niobium and yttrium. There appears to be a correlation between iron and actinolite content in the amphibole-rich samples, although this is somewhat obscured by the presence of iron and base metal sulphides, as indicated by elevated values for trace elements (S_t, Pb, Zn, Sb, Ag, Bi, Cd and Sn) in the actinolite-rich sample.

Carbonate alteration is represented by samples F93-10 44.1 (dolomite rich) and F93-10 49.3 (talc-sericite-biotite bearing), which are enriched in lime (to 24%) and magnesia (to 25%), and are also distinguished by high loss on ignition to 37%, and carbon up to 10%. As for amphibole-talc-rich samples, low values for the immobile oxides alumina and titania and the immobile elements (Zr, Y and Nb) probably indicate significant volume addition.

Plagioclase (± biotite) alteration is represented by samples F92-1 141.1 (with garnet), 166.4 (strong calcic plagioclase), 173.3 (weak, calcic plagioclase), F92-2 105.2 (patchy), and F93-10 69.7 (veinlets). Where most strongly developed, this alteration is characterized by high alumina (up to 21%) and titania (up to 0.72%), probably due to volume loss during the alteration, which at Sullivan is typified by complete leaching of the original detrital quartz and replacement by plagioclase of albitic composition (Leitch *et al.*, in preparation b). However, at Fors this alteration is more calcic, as evidenced by the lime values being roughly equal or greater than the soda (Table 1). Silica values vary from about 84% in the weakest plagioclase alteration down to 65% in the strongest alteration, correlating with the destruction of detrital quartz and replacement by plagioclase.

Magnesia values are low to very low (0.1% in massive plagioclase alteration) due to the almost complete absence of mafic minerals; potash is also lowest in the strongest plagioclase alteration due to the absence of mica (muscovite and biotite). Manganese tends to be low (0.25%); scattered anomalous values in arsenic (to 560 ppm) and tin (to 43 ppm) or tungsten (to 10 ppm) are not obviously explainable. Both the tin and tungsten analyses are by ICP, and therefore represent minimum values.

Biotite alteration is represented by samples F93-10 39.2 (with significant pyrrhotite) and 59.8 (biotite dominant). These samples are characterized by elevated potash values compared to the other samples in the suite (4 to 9%), relatively low soda (1.3 to 0.1%) and lime (1.7 to 0.8%) and moderate to low silica (66 to 41%). Magnesia and iron are elevated, up to 21% and 8%, respectively. Values for the immobile oxides (alumina and titania) and elements (Zr, Y, Nb) are about average for these sediments and thus indicate little or no volume change, in agreement with findings for biotite hornfelsed or granofels altered sediments at the Sullivan deposit (Leitch *et al.*, in preparation b).

Sericitization is represented by one sample (F92-1 7.2, rich in muscovite and biotite) which contains somewhat elevated potash (3.6%), iron (5%) and magnesia (3.7%) with normal to slightly depleted silica (68%), immobile oxides alumina and titania, and immobile elements (Zr, Y and Nb). Thus this type of alteration is probably characterized by relatively little volume change, as indicated at Sullivan (Leitch *et al.*, in preparation b).

Silicification (samples F92-1 63 and F93-10 73.2) is characterized by moderately high silica (76-81%) and low values for alumina and titania (possibly due to either the protolith being quartzite with low initial values for these oxides, or to volume change during alteration: Leitch *et al.*, in preparation b). All other oxides are also low except CaO (3-4%), possibly due to calcic plagioclase, and Fe_2O_3 due to variable sulphide (detected by S_t up to 1.27% and elevated Pb and Zn in the sample from F92-1). Elevated MnO in this sample, which is from massive, silicified quartzite immediately above the stratiform sulphides (Figure 2), is probably due to manganiferous garnet, as noted petrographically from 3 metres deeper in the hole. The other sample, from a silicified zone below a plagioclase-altered zone in F93-10, is not anomalous except for 1000 ppm arsenic.

FLUID INCLUSIONS

PETROGRAPHY

Although all samples were examined petrographically for fluid inclusions, only two containing fluid inclusions in veins were analysed microthermometrically. All samples examined were from the footwall, below the stratiform semimassive sulphide horizon, and thus could be expected to contain a record of mineralizing solutions that formed the stratiform body. As at the Sullivan deposit (Leitch, in preparation), fluid inclusions are restricted to vein quartz, carbonate and rarely epidote; visible inclusions are not found in the adjacent detrital quartz. This implies that the fluid inclusions are related to the mineralizing episode, and not merely samples of metamorphic fluids. Also as at Sullivan, no primary fluid inclusions were seen in the Fors samples. The majority of inclusions are found along trails, or healed fractures, that do not cross crystal boundaries and therefore are pseudosecondary (*i.e.*, they probably record fluids passing through the rocks during the formation of the deposit). Small (generally 1-2 μm) inclusions along through-going fractures are probably secondary, and were not subjected to further analysis.

The observed fluid inclusions are mostly type 2 (a and b; possibly c) and less commonly type 1 (classification used for the Sullivan deposit in Leitch, 1992b; Leitch, in preparation). The basic distinction between type 1 and 2 is that the former are halite-saturated (over 26 weight % NaCl equivalent, hereafter abbreviated as wt %) whereas the latter are undersaturated. However, both have similar major cations, as indicated by eutectic temperatures.

In quartz veins cutting plagioclase-altered samples (F92-1 166.5 and F92-2 176.9), pseudosecondary type 2a/b inclusions up to 10 microns in diameter, with rounded to irregular outlines, are confined to trails in the quartz and rarely calcite, and do not cross into adjacent plagioclase. Massive carbonate from F92-1 79.5 does not contain visible fluid inclusions.

Laminated tourmalinite with scattered garnet from F92-2 281.1 is cut by pyrrhotite-sphalerite-quartz-minor plagioclase-zoisite-muscovite veins, but none of the silicate minerals contains visible fluid inclusions. Clear to white quartz-calcite-pyrite veins, both bedding parallel and perpendicular, in fine, dark brown, laminated tourmalinite from 422 metres in the same hole contain only very fine (2 μm) secondary fluid inclusions. Black tourmalinite with abundant laminated pyrrhotite from 525 metres in the same hole is cut by quartz-clinozoisite veins. Quartz in these veins contains pseudosecondary type 1 and 2 inclusions with regular or negative crystal shapes up to 7 microns in diameter. The type 1 inclusions contain halite daughter crystals and vapour bubbles roughly equal in size, at 1.5 to 2 microns, indicating vapour to liquid, or V/L, ratios of about 10% by volume and salinities of up to 35 wt%; many also contain one or two other daughter minerals with relief higher than halite, and variable birefringence. These refringent daughter minerals remain unidentified. The clinozoisite crystals contain abundant highly irregular, possibly one-phase (liquid or vapour) inclusions and less common, regular shaped type 2 inclusions to 8 microns in diameter, with vapour bubbles up to 1.5 microns indicating V/L ratios of about 10%.

A quartz-pyrrhotite vein from a major network spanning 20 metres in F92-6 (sampled at 102.6 metres), hosted in biotite-plagioclase-pyrrhotite alteration, contains pseudosecondary type 2 inclusions up to 45 microns long with vapour bubbles up to 8 microns in diameter (rarely to 27 μm , probably indicating necking).

MICROTHERMOMETRY

Microthermometric measurements were only possible on two samples, F92-2 525 and F92-6 102.6. In F92-2 525,

most type 1 inclusions froze only with difficulty at about -70 to -90 °C, or froze on warming to about -80 to -90 °C. Eutectic (first melting) temperatures ranged from -63 to -72 °C, indicating significant concentrations of $CaCl_2$ in addition to NaCl (Davis *et al.*, 1990). Magnesium chloride may also be present, but cannot be confirmed from the available data. On further warming, complex melting events observed over the range -45 to -23 °C, with modes near -32 and -24 °C (Tm_1 and Tm_2), may indicate melting of salt hydrates (see below). Type 2a inclusions displayed similar freezing and eutectic temperatures. In F92-6 102.6 and F92-1 525, type 2b inclusions found along fractures apparently crossing fractures containing type 1 and type 2a inclusions froze around -40 to -47 °C and displayed eutectic temperatures in the same range. In F92-6 102.6, type 2b inclusions froze at about -40 to -47 °C, with eutectic temperatures in the range -37 to -50 °C whereas type 2c inclusions found along separate fractures displayed double freezing at -32 and -45°C, characteristic of fluids containing minor CO_2; eutectic temperatures were in the same range as for type 2b. The higher eutectic temperatures for type 2b and c inclusions suggest that although magnesium may be present in these fluids, calcium is not likely.

Salinities of the inclusion fluids were estimated by temperature of dissolution of the halite cube (Ts) for type 1 inclusions, modified by temperature of melting events 1, 2 and final (Tm_1, Tm_2, Tm_f) in type 1 and 2a/b inclusions; for type 2c inclusions, by final melting temperatures modified by clathrate melting (Tm_c) where observed. For Ts values in the 220 to 464°C range, salinities of 32-47 wt% NaCl equivalent are indicated (Roedder, 1984). However, due to the "salting out" effect caused by divalent salts, these values may overestimate the salinity (Roedder, 1984). These inclusions can be best understood in the context of ternary NaCl-$CaCl_2$-H_2O and $MgCl_2$-$CaCl_2$-H_2O diagrams (Crawford, 1981). Intermediate melting temperatures Tm_1 and Tm_2 were difficult to observe in the presence of other solids (ice and/or hydrohalite), but where measured were in the ranges -35 to -45 °C and -24 to -29 °C respectively. The less common event at -35 to -45 °C is interpreted as the melting of a phase such as $CaCl_2.6H_2O$ or $MgCl_2.12H_2O$ (Crawford *et al.*, 1979), and suggests a wide range of the magnesium to calcium ratio in the fluid, possibly due to both elements being present in small amounts in these cases. Melting in the range -24 to -26 °C was much more common; in type 1 (halite-bearing) inclusions, this appeared to be final ice melting, whereas in type 2a/b inclusions, this is interpreted as hydrohalite melting in the presence of ice. In either case, the temperature serves to fix the Na/Ca ratio of the fluid at about 1:1 (or X_{NaCl} of 0.5; less commonly between 0.35 and 0.7).

Salinity estimates can best be made by comparing final ice-melting temperatures to a ternary NaCl-$CaCl_2$-H_2O diagram (Crawford, 1981; *cf.* Peter *et al.*, 1994). Final melting temperatures are between -8.5 and -23 °C for type 2a/b inclusions, giving salinities from 15-20 wt% . For type 2c inclusions, final melting temperatures between -0.2 and -10.6°C indicate relatively low salinities (3 to 13 wt%; Potter *et al.*, 1978). However, these are probably overestimates for the salinities, due to the withdrawal of water into clathrates (Collins, 1979). Clathrate melting is common in type 2c inclusions but rare in type 2a or b; it is not seen in type 1 inclusions. Clathrate melting temperatures mainly in the 6 to 7°C range indicate salinities less than 10 wt%, possibly slightly overestimated by the presence of CH_4 in addition to CO_2 (Roedder, 1984).

Homogenization temperatures (vapour to liquid) are difficult to measure for these inclusions, due to stretching and decreptitation, but in sample F92-2 525, the range for type 1 and type 2a inclusions is from 125 to 285°C and for type 2b from 98 to 250°C. In sample F92-6 102.6, the range for type 2b is from 260 to 371°C and for type 2c is from 202 to 290°C. As at the Sullivan deposit (Leitch, in preparation) interpretation of seawater depths of 1500 to 2000 metres leads to trapping temperatures for type 1 and 2a inclusions of 150 to 300°C. However, type 2b inclusions in quartz-pyrrhotite veins at Fors appear to record higher temperatures of up to 395°C, possibly reflecting late main-stage overprinting in the well developed vent zone, correlative with the second pulse that produced veins enriched in arsenic, tungsten, silver and bismuth (Britton and Pighin, 1995). Although not subjected to microthermometry, fluid inclusions associated with plagioclase alteration at Fors (possibly similar to albitic alteration at Sullivan) may also record similar or lower temperatures than the main-stage alteration (Leitch, in preparation).

DISCUSSION

One of the key questions at the Fors deposit concerns the setting of the mineralization and whether it differed from that of the Sullivan deposit. Certain features such as the form and distribution of the tourmalinites (black bedded and brown replacing fragmental rocks), and the unusual calcsilicate cap rock, bear on this question.

On the basis of preliminary evidence, tourmaline from the Fors deposit appears to be generally slightly more iron rich than tourmaline at the Sullivan deposit, at least in the black, commonly laminated tourmalinite interbedded with siltstone near the lower to middle Aldridge contact (Figure 2). It is also not clear from the limited analytical work of this study that the tourmaline in brown tourmalinite, commonly observed replacing fragmental rock, is richer in magnesium (as suggested by Britton and Pighin, 1995 and Slack, 1993). Various authors have suggested that increased magnesium content of the hydrothermal tourmaline is favourable for mineralization (*e.g.*, Taylor and Slack, 1984).

It is not clear whether the dark laminated tourmalinite at Fors formed syngenetically on the seafloor, or by replacement of previously formed sediments; although Slack (1993) generally favours the latter, either case is permissive of a brine-pool setting. The absence of detrital quartz, and the presence of anomalous apatite and native bismuth in the sphalerite (±galena)-rich laminae of this tourmalinite, suggests that some of these layers are true chemical precipitates. Although the sieve texture of the garnets in tourmalinite implies that they grew during metamorphism,

their high manganese content suggests they grew from a manganese-rich precursor such as carbonate or hydroxide, as at the Sullivan deposit, where such manganese content is taken to indicate the presence of a brine pool.

The calcsilicate caprock is composed of layers rich in amphibole (tremolite to actinolite), talc, carbonate, plagioclase and micas (biotite and muscovite). The magnesium-rich nature of this alteration assemblage suggests it may have formed in response to mixing with downward-welling, magnesium-rich seawater in the footwall, as the system cooled after deposition of the main stratabound sulphide horizon, possibly at the top of the feeder pipe now represented by the tourmalinized fragmental. However, the shape of the calcsilicate cap is suggestive of a mound that could have formed over the top of a vent debouching on the seafloor. In this scenario, stratiform semimassive sulphides would have had to form after the calcsilicate mound.

Absence of the detrital quartz framework in calcsilicate alteration zones suggests they are derived from a different protolith than most of the host clastic sediments, possibly from chemical sediments; alternatively, the original framework may have been totally leached during alteration. Complete leaching of the quartz framework of the hostrocks is well documented at Sullivan, where both chloritized and albitized rocks containing no quartz can be traced into sediments with abundant detrital quartz. At Fors, significant volume addition for samples rich in amphibole, talc and carbonate may indicate swamping of the normal detrital sediment input by a chemical precipitate, either in a hydrothermal mound or a brine-pool setting.

The abundance of calcic plagioclase in the Fors alteration is distinct from the albite so common at Sullivan, and demands an explanation. Possibly there was so much calcium, either derived from the calcsilicate chemical sediment or alteration, floating around in the system that during metamorphism the calcic plagioclase had to form, much as in the metamorphism of a calcsilicate. The timing of plagioclase alteration is also uncertain, but it does not appear to be as late as at the Sullivan, as plagioclase envelopes to tourmalinite veins are seen. Possibly there was more overlap between the tourmalinite and plagioclase alteration phases, or a later pulse of tourmalinite (veining) is present.

As at the Sullivan deposit (Leitch *et al.* in preparation a), sericite alteration appears to form a general envelope to the main mineralized zones at the Fors deposit. Timing of this alteration is difficult to establish, particularly on the basis of petrographic relationships, as at Sullivan. Sericitization of albite-oligoclase envelopes to tourmaline veins does not necessarily suggest sericite is later than albite as only fine (possibly detrital) feldspar is replaced.

Hydrothermal fluids associated with tourmalinite formation, and possibly responsible for the Fors lead-zinc mineralization, appear to have been broadly similar to those at the Sullivan deposit: highly saline (halite saturated to just undersaturated) and containing significant calcium in addition to sodium. Similar fluids are found in the Iron Creek copper-cobalt-gold deposit in Idaho (Leitch and Hall, in preparation) and similar or less saline fluids are found in the Sheep Creek copper-cobalt deposit in Montana (Leitch *et al.*, in preparation c; Zieg and Leitch, 1994). The mineralizing fluids may have been at about 150 to 300°C, similar to temperatures for the Sullivan type 1 - type 2a fluids (Leitch and Turner, 1992; Leitch, in preparation). However, at Fors, there is a suggestion of hotter post-main stage fluids trapped at up to 395 °C in type 2b inclusions in quartz-pyrrhotite veins associated with arsenopyrite, scheelite, and silver-bismuth values. Eutectic temperatures suggest these fluids may have contained magnesium rather than calcium in addition to sodium, inviting the suggestion that they were also associated with the magnesium-rich calcsilicate cap over the deposit. Possibly the magnesium could have been supplied by downward circulation of seawater that mixed with the post-main stage fluids.

By comparison with studies at Sullivan and other localities elsewhere in the Aldridge Formation (Leitch, in preparation), the more dilute fluids containing traces of carbonic fluid (type 2c inclusions) are probably related to Mesozoic metamorphism.

REFERENCES

Anderson, H.E., Goodfellow, W.D. and Parrish, R.R. (in preparation): U-Pb Geochronology, Petrogenesis and Tectonic Setting of the Middle Proterozoic Moyie Sills, Purcell Basin, B.C.; *Geological Survey of Canada*, Special Volume.

Britton, J.M. and Pighin, D.L. (1995): Fors - a Proterozoic Sedimentary Exhalative Base Metal Deposit, Purcell Supergroup, Southeastern British Columbia (82G/5W); *in* Geological Fieldwork 1994, Grant, B. and Newell, J.M., Editors, *B.C. Ministry of Energy, Mines and Petroleum Resources*, Paper 1995-1, pages 99-109.

Collins, P.L.F. (1979): Gas Hydrates in CO_2-bearing Fluid Inclusions and the Use of Freezing Data for Estimation of Salinity; *Economic Geology*, Volume 74, pages 1435-1444.

Crawford, M.L. (1981): Phase Equilibria in Aqueous Fluid Inclusions; *in* Fluid Inclusions: Applications to Petrology, *Mineralogical Association of Canada*, Short Course Handbook Volume 6, pages 75-100.

Crawford, M.L., Kraus, D.W. and Hollister, L.S. (1979): Petrologic and Fluid Inclusion Study of Calc-silicate Rocks, Prince Rupert, British Columbia; *American Journal of Science*, Volume 279, pages 1135-1159.

Davis, D.W., Lowenstein, T.K. and Spencer, R.J. (1990): Melting Behavior of Fluid Inclusions in Laboratory-grown Halite Crystals in the Systems NaCl-H_2O, NaCl-KCl-H_2O, NaCl-$MgCl_2$-H_2O, and NaCl-$CaCl_2$-H_2O; *Geochimica et Cosmochimica Acta*, Volume 54, pages 591-601.

De Paoli, G.R. and Pattison, R.M.D. (1994): Metamorphic Pressure, Temperature, and Fluid Conditions of the Sullivan Mine, Kimberley, British Columbia, Using Silicate-Carbonate Equilibria (abstract); *in* Minerals Colloquium, Program with Abstracts, Ottawa, Ontario, January 17-19, *Geological Survey of Canada*, unpaginated.

Edmunds, F.R. (1977): The Aldridge Formation, B.C., Canada; unpublished Ph.D. thesis, *Pennsylvania State University*, University Park, Pennsylvania, 368 pages.

Holland, R.A.G., Rey, C.J. and Spooner, E.T.C. (1978): A Method for Preparing Doubly Polished Thin Sections Suitable for Microthermometric Examination of Fluid Inclusions; *Mineralogical Magazine*, Volume 42, pages 407-408.

Höy, T., (1989): The Age, Chemistry, and Tectonic Setting of the Middle Proterozoic Moyie Sills, Purcell Supergroup, Southeastern British Columbia; *Canadian Journal of Earth Sciences*, Volume 26, pages 2305-2317.

Höy, T. (1993): Geology of the Purcell Supergroup in the Fernie West-half Map Area, Southeastern British Columbia; *B.C. Ministry of Energy, Mines and Petroleum Resources*, Bulletin 84, 157 pages.

Höy, T. and Pighin, D.L. (1995): Vine - a Middle Proterozoic Massive Sulphide Vein System, Purcell Supergroup, Southeastern British Columbia (82G/5W); *in* Geological Fieldwork 1994, Grant, B. and Newell, J.M., Editors, *B.C. Ministry of Energy, Mines and Petroleum Resources*, Paper 1995-1, pages 85-98.

Klewchuck, P. (1993): Assessment Report on Two Diamond Drill Holes (F92-2 & 3), Fors Property; *B.C. Ministry of Energy, Mines and Petroleum Resources*, Assessment Report 22817.

Leitch, C.H.B. (1992a): Mineral Chemistry of Selected Silicates, Carbonates, and Sulphides in the Sullivan and North Star Stratiform Zn-Pb Deposits, British Columbia, and in District-scale Altered and Unaltered Sediments; *in* Current Research, Part E, *Geological Survey of Canada*, Paper 92-1E, pages 83-93.

Leitch, C.H.B. (1992b): A Progress Report of Fluid Inclusion Studies of Veins from the Vent Zone, Sullivan Stratiform Sediment-hosted Zn-Pb Deposit, B.C.; *in* Current Research, Part E, *Geological Survey of Canada*, Paper 92-1E, pages 71-82.

Leitch, C.H.B. (in preparation): Fluid Inclusion Studies of the Sullivan Sttratiform Sediment-hosted Zn-Pb Deposit, British Columbia; *Geological Survey of Canada*, Special Volume.

Leitch, C.H.B. and Hall, S.M. (in preparation): Main Copper Zone of the Iron Creek Stratabound Sediment-hosted Cu-Co Deposit, Idaho Cobalt Belt, Lemhi County, Idaho: Fluid Inclusion and Related Studies; *Geological Survey of Canada*, Special Volume.

Leitch, C.H.B. and Turner, R.J.W. (1992): Sulphide-bearing Network Underlying the Western Orebody, Sullivan Stratiform Sediment-hosted Zn-Pb Deposit, B.C.: Preliminary Field, Petrographic and Fluid Inclusion Studies; *in* Current Research, Part E, *Geological Survey of Canada*, Paper 92-1E, pages 61-70.

Leitch, C.H.B., Turner, R.J.W. and Höy, T. (1991): The District-scale Sullivan - North Star Alteration Zone, Sullivan Mine Area, British Columbia: A Preliminary Petrographic Study; *in* Current Research, Part E, *Geological Survey of Canada*, Paper 91-1E, pages 45-57.

Leitch, C.H.B., Turner, R.J.W., Shaw, D.R., Hodgson, C.J. and Brown, T. (in preparation, a): Evolution of the Vent Complex, Sullivan Stratiform Sediment-hosted Zn-Pb-Ag Deposit: Part 2, Wall-rock Alteration and Sulphide Mineralization; *Geological Survey of Canada*, Special Volume.

Leitch, C.H.B., Turner, R.J.W., Ross, K.V., Shaw, D.R. and Höy, T. (in preparation, b): Lithogeochemistry of Altered Wallrocks, Sullivan Stratiform Sediment-hosted Zn-Pb-Ag Deposit; *Geological Survey of Canada*, Special Volume.

Leitch, C.H.B., Zieg, G.A. and Hall, S.M. (in preparation, c): Preliminary Fluid Inclusion and Stable Isotope Studies of the Sheep Creek Stratabound Sediment-hosted Cu-Co Deposit, Meagher County, Montana; *Geological Survey of Canada*, Special Volume.

Lydon, J.W. and Reardon, N. (1994): Sphalerite Compositions of the Sullivan Deposit, British Columbia and their Implications for Timing of Metamorphism (abstract); *in* Minera s Colloquium, Program with Abstracts, Ottawa, Ontario, January 17-19, *Geological Survey of Canada*, unpaginated.

Maheux, P.J. (1990): Geology and Geochemistry Report on the Fors Property, Puma and Cougar Claims; *B.C. Ministry of Energy, Mines and Petroleum Resources*, Assessment Report 19809.

McMechan, M.E. and Price, R.A. (1982): Superimposed Low-grade Metamorphism in the Mount Fisher Area, Southeastern British Columbia—Implications for the East Kootenay Orogeny; *Canadian Journal of Earth Sciences*, Volume 19, pages 476-489.

Peter, J.M., Goodfellow, W.D. and Leybourne, M.I. (1994): Fluid Inclusion Petrography and Microthermometry of the Middle Valley Hydrothermal System, Northern Juan de Fuca Ridge; *in* Proceedings of the Ocean Drilling Program, Scientific Results, Mottl, M.J., Davis, E.E., Fisher, A.T. and Slack, J.F., Editors, Volume 139, pages 411-428

Potter, R.W., Clynne, M.A. and Brown, D.L. (1978): Freezing Point Depression of Aqueous Sodium Chloride Solutions; *Economic Geology*, Volume 73, pages 284-285.

Price, R.A. (1981): The Cordilleran Foreland Thrust and Fold Belt in the Southern Canadian Rocky Mountains; *in* Thrust and Nappe Tectonics, McClay, K.R. and Price, R.A., Editors, *The Geological Society of London*, pages 427-448.

Roedder, E. (1984): Fluid Inclusions; *Mineralogical Society of America*, Reviews in Mineralogy, Volume 12, 644 pages.

Schandl, E.S., Davis, D.W. and Gorton, M.P. (1993): The Pb-Pb Age of Metamorphic Titanite in the Chlorite-Pyrite Altered Footwall of the Sullivan Zn-Pb Sedex Deposit, B. C. and its Relationship to the Ore (abstract); *Geological Association of Canada - Mineralogical Association of Canada*, Program with Abstracts, Volume 18, page A93.

Shaw, D.R., Hodgson, C.J., Leitch, C.H.B. and Turner, R.J.W. (1993a): Geochemistry of Tourmalinite, Muscovite, and Chlorite-Garnet-Biotite Alteration, Sullivan Zn-Pb Deposit, British Columbia; *in* Current Research, Part A, *Geological Survey of Canada*, Paper 93-1A, pages 97-107.

Shaw, D.R., Hodgson, C.J., Leitch, C.H.B. and Turner, R.J.W. (1993b): Geochemistry of Albite-Chlorite-Pyrite and Chlorite-Pyrrhotite Alteration, Sullivan Zn-Pb Deposit, British Columbia; *in* Current Research, Part A, *Geological Survey of Canada*, Paper 93-1A, pages 109-118.

Slack, J.F. (1993): Models for Tourmalinite Formation in the Middle Proterozoic Belt and Purcell Supergroups (Rocky Mountains) and their Exploration Significance; *in* Current Reserarch, Part E; *Geological Survey of Canada*, Paper 93-1E, pages 33-40.

Taylor, B.E. and Slack, J.F. (1984): Tourmalines from Appalachian-Caledonian Massive Sulphide Deposits: Textural, Chemical, and Isotopic Relationships; *Economic Geology*, Volume 79, pages 1703-1726.

Winston, D., Woods, M. and Byer, G.B. (1984): The Case for an Intracratonic Belt-Purcell Basin: Tectonic, Stratigraphic and Stable Isotope Considerations; *Montana Geological Society*, 1984 Field Conference, pages 103-118.

Zieg, G.A. and Leitch, C.H.B. (1993): The Geology of the Sheep Creek Copper Deposits, Meagher County, Montana, Program and Abstracts, Belt Symposium III, August 14-21, *Belt Association Inc.*, Spokane.

NOTES